ResearchGate

See discussions, stats, and author profiles for this publication at: https://www.researchgate.net/publication/231699321

Asymmetric Curvature of Growth Faces of Polymer Crystals

ARTICLE *in* MACROMOLECULES · JANUARY 2007

Impact Factor: 5.8 · DOI: 10.1021/ma0617872

CITATIONS
6

READS
14

2 AUTHORS:

Maxim Shcherbina
Institute of Synthetic Polymeric Materials
50 PUBLICATIONS **300** CITATIONS
SEE PROFILE

Goran Ungar
The University of Sheffield
279 PUBLICATIONS **10,058** CITATIONS
SEE PROFILE

Available from: Maxim Shcherbina
Retrieved on: 26 January 2016

Asymmetric Curvature of Growth Faces of Polymer Crystals

M. A. Shcherbina and G. Ungar*

Department of Engineering Materials, University of Sheffield, Sheffield S1 3JD, U.K.

Received August 7, 2006
Revised Manuscript Received December 14, 2006

Lamellar polymer crystals often have curved lateral growth faces.[1,2] Understanding such morphology is of major interest since it allows the distinction between fundamentally different theories of polymer crystallization.[3−6] For example, Sadler's "roughness-pinning" theory[4] originated from the assumption that the curvature is a consequence of the roughening transition on selected lateral growth faces. The complex pattern of crystal rounding has also been attributed to the roughening transition in *n*-alkanes with 20−30 carbons.[7] Mansfield,[8] Point and Villers,[9] and Toda[10] have since shown that the curvature in polymers can be quantitatively explained essentially within the framework of the Frank−Seto[11,12] model of crystal growth, which postulates nucleation and spreading rates of steps on the growth face but makes no attempt to explain these rates. Kyu et al. computed the growth habit of PE crystals using a nonlinear reaction diffusion equation where the crystal−melt interface was diffuse rather than sharp.[13]

In refs 8−10 the Frank−Seto model[11,12] of crystal growth was applied, which defines i as the rate of formation of surface nuclei (nuclei per unit edge length per time) and v as the average net rate of travel of the generated steps along the growth surface (in units of length per time). $l(x,t)$ and $r(x,t)$ are then the densities of left and right steps, respectively, in the vicinity of position x on the surface. Since steps are generated by nucleation and annihilated by collision, two flux equations must be satisfied:[11,12]

$$\frac{\partial r}{\partial t} = -v\frac{\partial r}{\partial x} + i - 2vlr \tag{1a}$$

$$\frac{\partial l}{\partial t} = +v\frac{\partial l}{\partial x} + i - 2vlr \tag{1b}$$

If no steps enter from outside, and the ends of the crystal face move outward at a rate h, the boundary conditions for eqs 1 are $r(-ht,t) = l(ht,t) = 0$.

Mansfield[8] has solved the above equations for a simple square lattice and obtained the growth face profile $y(x,t)$ in the form of an ellipse, in the large-crystal approximation. The ellipse becomes leaf-shaped when transposed onto a polyethylene-like centered rectangular lattice.[14] The {100} face in observed polyethylene (PE)[14] and long-alkane[15] crystals is well described as part or whole of this modified ellipse if the substrate ends move respectively at a rate $h < v$ ("truncated lozenge") or $h = v$ ("lenticular" crystal).

Implicit in the above is the fact that, for crystal faces to be visibly curved, v must be substantially slower than predicted by the LH theory. The retardation appears to be due to the "self-poisoning" or "pinning" effect of incorrect chain attachment, starkly demonstrated by the extreme cases of growth rate minima in long-chain alkanes.[16]

* Corresponding author. E-mail: g.ungar@shef.ac.uk.

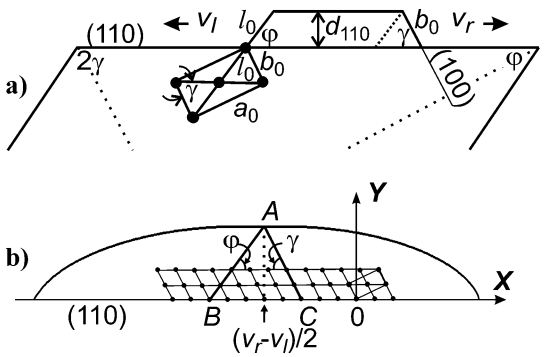

Figure 1. (a) Schematic view along the chain axis of a new molecular layer deposited on a 110 growth face of a PE or PVDF crystal showing the asymmetry of steps. The right and left steps would have been equivalent if the lattice had hexagonal symmetry ($a_0/b_0 = \sqrt{3}$). (b) Transposing the solution for the growth front of an asymmetric crystal face from the simple square lattice onto the oblique lattice appropriate for a {110} growth face. a_0/b_0 ratio is for PVDF (α-form). A unit cell is shown for reference in both (a) and (b).

Recently, solution-grown crystals of alkanes such as *n*-$C_{162}H_{326}$ or *n*-$C_{198}H_{398}$ have been found with unusual habits ("*a*-axis lenticular") that can be best described as bounded by curved {110} faces.[17] The interesting feature is the asymmetry of the curvature: while the faces are curved at the obtuse apex, they are almost straight at the acute apex. We suggested that the key to understanding the curvature of {110} faces is to assume that the rates of propagation to the left and to the right are different (see Figure 1a). In fact, there is no reason to assume that $v_l = v_r$ for a crystallographic face (such as {110}) that lacks a symmetry plane bisecting it normal to the lamella, a 2-fold axis normal to it, or an associated glide plane or screw axis.

The problem is general and applies to all cases where crystal growth can be approximated as two-dimensional and where the growth face lacks mirror symmetry. Mathematical analysis of the curvature of asymmetric faces has been carried out on a simple square lattice using a modified Frank model.[18] In this Communication we show on selected examples that the solution, when adapted to the appropriate 2D lattices, indeed matches the observed but unexplained shapes of crystals of long alkanes and poly(ethylene oxide) (PEO). A good match is also obtained[19] for "*a*-axis lenticular" crystals of poly(vinylidene fluoride) (PVDF).[20] The method allows determination of kinetic parameters i, v_r, and v_l.

In order to treat cases where $v_r \neq v_l$, eqs 1 must be modified to

$$\frac{\partial r}{\partial t} = -v_r\frac{\partial r}{\partial x} + i - (v_r + v_l)lr \tag{2a}$$

$$\frac{\partial l}{\partial t} = +v_l\frac{\partial l}{\partial x} + i - (v_r + v_l)lr \tag{2b}$$

Assuming that the spreading rates of left and right substrate edges h_l and h_r can differ, we have solved[18] the system of differential equations (2) with the boundary conditions $r(-h_l t,t) = 0$ and $l(h_r t,t) = 0$. The resulting functions $r(x,t)$ and $l(x,t)$ were used in the reconstruction of the shape of the growth face on the simple square lattice by integration of the mean slope of the growing face given by $\partial y/\partial x = b(l - r)$, where b is the

10.1021/ma0617872 CCC: $37.00 © 2007 American Chemical Society
Published on Web 01/06/2007

width of a single chain (side of the unit square). This gives for the profile of the growth front

$$\left[\frac{X_s - (v_r - v_l)/2}{(v_r + v_l)/2}\right]^2 + \left[\frac{Y_s}{b\sqrt{i(v_r + v_l)}}\right]^2 = 1 \qquad (3)$$

where $X_s = x/t$ and $Y_s = y/t$ are time-independent coordinates on the square lattice. The shape of (3) is similar to that of the Mansfield ellipse but is shifted along the X-axis depending on the value of $(v_r - v_l)/2$.

In order to apply the solution (3) to the {110} growth faces in PE, alkanes, and PVDF, it has to be transposed onto an oblique lattice (see Figure 1b). This is because the sides of the kinks on the (110) face, rather than being parallel to Y, are parallel to densely packed planes (100) and $(\bar{1}10)$, inclined to X at angles γ and φ, respectively. With reference to Figure 1b, for the two branches of the growth front either side of the maximum at $X = (v_r - v_l)/2$, the corrected coordinate X_{ob} is given by eq 4, while $Y_{ob} = (d_{110}/l_0)Y_s$.

$$X_{ob} = X_s - [d_{110}\sqrt{i(v_r + v_l)} - Y_{ob}] \cot \varphi \qquad \text{if } X < \frac{v_r - v_l}{2}$$

$$X_{ob} = X_s + [d_{110}\sqrt{i(v_r + v_l)} - Y_{ob}] \cot \gamma \qquad \text{if } X \geq \frac{v_r - v_l}{2} \qquad (4)$$

Here d_{110} is the {110} interplanar spacing, while l_0 will generally denote the interchain distance in the crystallographic growth plane.

In order to compare the calculated profiles with the observed shapes of {110}-bounded crystals of alkanes, PE and PVDF ("lozenges"), we construct the full crystal shapes as illustrated in Figure 2a,b. A library of such shapes is generated with two systematically varied dimensionless ratios as parameters: $il_0^2/(v_r + v_l)$ and v_r/v_l (see Figure 3). The parameter $il_0^2/(v_r + v_l)$ gives the ratio of probabilities of deposition of a stem as a surface nucleus vs that of its attachment to a niche on either side of an existing layer. Observed crystal shapes are then compared to calculated ones in order to obtain the above two kinetic parameters.

In the construction in Figures 2a,b four {110} faces grow from a common center. The two crossed dotted lines define the baselines ($t = 0$) or X-axes. For a low initiation-to-propagation ratio, the growth faces are straight and parallel to their baseline (Figure 2a), maintaining crystallographic angles at the apices. As $il_0^2/(v_r + v_l)$ increases, the faces become curved and the apex angles change (see Figure 2b). Figure 3 illustrated the possible variation in apex angles and the existence of "noncrystallographic facets" when $v_l \neq v_r$. It also demonstrates how corners can be completely rounded and even made reentrant (i.e., concave—see crystal at bottom left).

Figure 4a−d shows actual crystals of n-$C_{162}H_{326}$ grown from 1-phenyldecane, bounded solely by {110} faces; the curvature is seen to decrease with increasing ΔT. In PE, crystals with complete and curved {110} faces are not observed, since at high crystallization temperature (T_c) where curvature is normally seen, the lozenge crystals are truncated by the slow growing {100} faces. The reason for this not being the case in alkanes is believed to be the lack of "self-poisoning" at low ΔT, as discussed elsewhere.[16,17] As seen in Figure 4, calculated crystal habits give excellent fits to the observed crystal shapes. Equally good fits are obtained[19] for PVDF crystals presented in ref 20.

Much morphological work has been done on melt-grown single crystals of narrow molecular fractions of PEO.[21,22] The

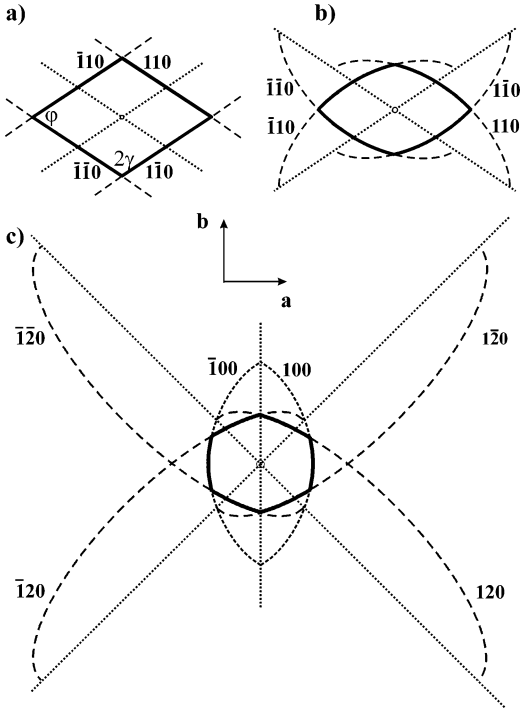

Figure 2. Construction of crystal shape bounded by four (a) straight {110} and (b) curved {110} growth faces (alkane/PE lattice parameters are used); (c) construction of the shape of a PEO crystal bounded by {120} and {100} faces. Bold lines are growth fronts intersecting at crystal corners, while dotted lines are reference ($t = 0$) baselines. Boundaries of the faceted lozenge crystal in (a) are parallel to the baselines. The curved growth profile in (b) was calculated using eqs 3 and 4 with parameters $il_0^2/(v_r + v_l) = 0.1$ and $v_r/v_l = 2$. For {120} faces in (c) $il_0^2/(v_r + v_l) = 0.125$ and $v_r/v_l = 5$, while for {100} faces Mansfield equation was used, adapted for PEO lattice, with $il_0^2/2v = ia_0^2/8v = 0.25$.

examples in Figure 4e−g are quite representative of such crystals and show two interesting features: (i) pronounced changes in habit, from faceted to circular and back, in a narrow range of ΔT, and (ii) the appearance of facets, seemingly {140}, that are not densely packed planes. In contrast, dilute solution-grown single crystals of PEO are bounded by {100} and {120} facets, both densely packed (see the shape inscribed in the crystal in Figure 4e).[23] Both features (i) and (ii) have been puzzling researchers for some time.[21,22] The present mathematical description of the habits helps explain these peculiarities.

As the fits in Figure 4e,g show, the apparent {140} facets are in fact {120} growth faces with steps traveling toward the outlying {100} faces 4 times faster than away from them. This causes a pileup of growing layers toward the borders with {100} faces, causing the {120} faces to tilt. In contrast, crystals that grow from dilute solution tend to have a low initiation-to-propagation ratio and thus display crystallographic facets, the difference between v_l and v_r being immaterial.

It appears to be a general trend, seen in alkanes, PVDF, and PEO crystals, that the asymmetry of step spreading rate is the highest at the lowest supercooling. As ΔT increases, v_r/v_l tends toward 1 (see, e.g., Figure 4a−d). This is understandable: at the melting (dissolution) temperature (T_m, T_d) molecular attachment and detachment rates are balanced, and any small difference in kinetic conditions between the right and left step would have greatest impact near T_m (T_d). It can be shown that the binding energy of chains attached at the right and left steps on a {110} face in, e.g., PE are equal. Since v is the difference between attachment and detachment rates, it follows that the difference between v_l and v_r is due to the difference in

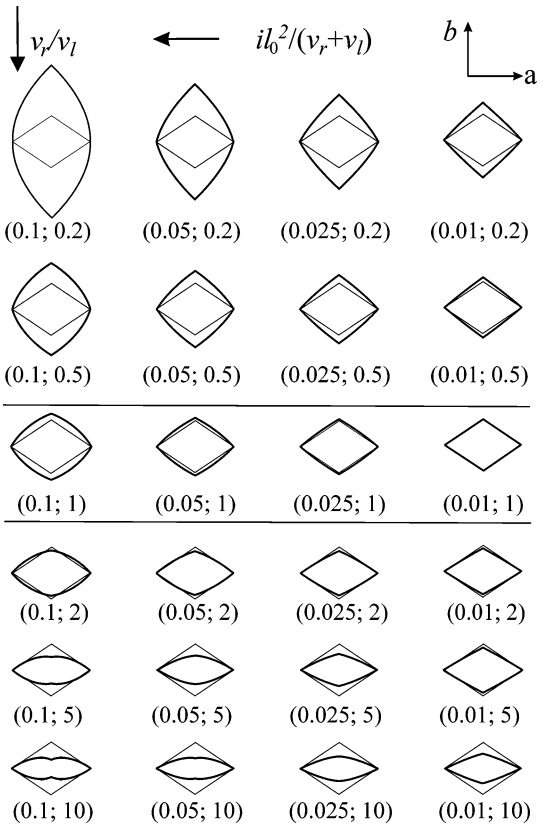

Figure 3. Library of constructed shapes of polyethylene crystals bounded by {110} faces. Columns: shapes with the same initiation/propagation rate ratio $il_0^2/(v_r + v_l)$; rows: shapes with the same right/left propagation rate ratio v_r/v_l. For comparison, crystallographic lozenges with the same size in the *a* direction are shown (thin lines). The corresponding kinetic parameters are shown beneath each simulated crystal in the form ($il_0^2/(v_r + v_l)$; v_r/v_l).

attachment rates at the two nonequivalent ends of a growing layer. However, as supercooling increases, attachment becomes less selective and $v_r/v_l \rightarrow 1$. In Figure 4a−d v_r/v_l changes from 2.8 to 1 as ΔT increases from 2.6 to 8.7 °C. However, in the PEO crystals in Figure 4, parts e and g, v_r/v_l has virtually the same value of 4 in spite of the difference in ΔT. This is because the crystal in Figure 4g is a folded-chain crystal formed immediately below the extended-folded chain growth transition; hence, its ΔT should be considered relative to T_m of folded-chain crystals.

Parts e and f of Figure 4 show only selected examples of a series of crystals grown at 1 °C intervals.[22] Their analysis shows a monotonous increase in $il_0^2/(v_r + v_l)$ and a decrease toward unity in v_r/v_l as T_c decreases to the folded-chain growth transition. The initiation/propagation ratio $ib_0^2/2v$ for {100} similarly shows an increase. Reevaluating growth rate data by Kovacs et al.,[21] one realizes that retardation in extended-chain growth takes place close to the folded-chain transition. This is attributed to self-poisoning,[16,24] i.e., growth surface obstruction by frequent but unstable folded-chain depositions. The fact that in PEO the initiation-to-propagation ratio increases on both {120} and {100} faces as T_c approaches the transition shows that the disruption of step propagation is more pronounced than that of step initiation. This is exactly the opposite of the situation in long alkanes where, particularly in solution growth, crystals become needlelike and faceted near the folded-chain transition, with $ib_0^2/2v \rightarrow 0$, i.e., initiation virtually coming to a halt.[15,16]

It is also worth noting that with $il_0^2/(v_r + v_l) = 0.5$ (Figure 4f), i.e., the probability of a chain acting as nucleus being as much as half the probability of it attaching to an existing step, the growth process effectively ceases to be nucleation controlled and approaches the rough-surface growth mechanism of Sadler.[4] A similar situation occurs in long alkane crystals growing halfway between the extended- and folded-chain dissolution temperatures.[15] It should be noted that theoretical treatments based on the Frank−Seto model, such as the present one, become only semiquantitative for dimensionless i/v ratios above 0.1.[11]

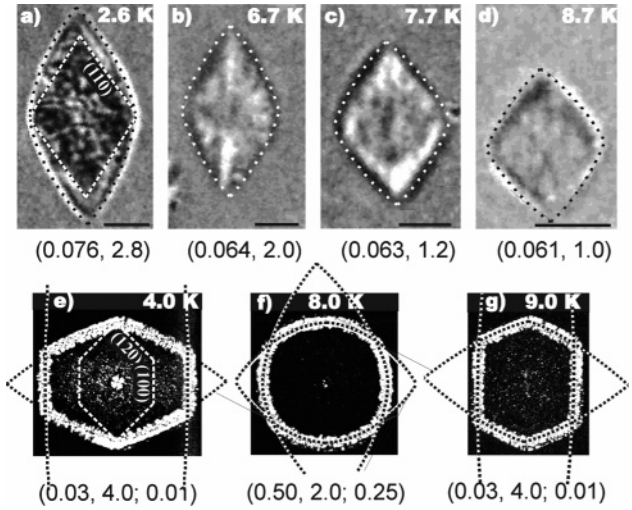

Figure 4. Optical micrographs (a−d) of single crystals of long alkane $C_{162}H_{326}$ grown from 1 wt % solution in 1-phenyldecane (from ref 17, scale bar 10 μm) and (e−g) of methyl-terminated PEO ($M_w = 3050$, $M_w/M_n = 1.02$) melt-grown crystals (from ref 22). Supercoolings (ΔT) relative to the melting/dissolution temperature of the extended-chain form is indicated. The crystallographic *a*-axis is vertical in (a−d), but horizontal in (e−g) as well as in Figures 2 and 3. Crystals (a−f) are extended-chain, and (g) is once-folded chain. Dotted lines: fitted profiles using eqs 3 and 4 for {110} and {120} faces and using corrected Mansfield ellipse[14] for {100} faces. Fitting parameters are shown in (a−d) as ($il_0^2/(v_r + v_l)$, v_r/v_l) and in (e−g) as ($il_0^2/(v_r + v_l)$, v_r/v_l; $ib_0^2/2v$), the first two ratios for {120} and the third for {100}. A faceted outline is inscribed in crystals (a) and (e).

The work described here helps explain a number of hitherto poorly understood polymer morphologies (alkanes, PVDF, PEO) and temperature-induced morphological changes. In principle, it allows independent measurements of step initiation and propagation rates on all growth faces of lamellar polymer crystals. However, understanding the asymmetry of step propagation and the $il_0^2/(v_r + v_l)$ ratio on molecular level is an open challenge.

Acknowledgment. Financial support from Engineering and Physical Science Research Council is acknowledged.

References and Notes

(1) Keith, H. D. *J. Appl. Phys.* **1964**, *35*, 3115.
(2) Khoury, F. *Faraday Discuss. Chem. Soc.* **1979**, *68*, 404.
(3) Hoffman, J. D. *Polymer* **1997**, *38*, 3151.
(4) Sadler, D. M. *Polymer* **1983**, *24*, 1401.
(5) Welch, P.; Muthukumar, M. *Phys. Rev. Lett.* **2001**, *87*, 218302.
(6) Heck, B.; Strobl, G.; Grasruck, M. *Eur. Phys. J. E* **2003**, *11*, 117.
(7) Liu, X. Y.; Bennema, P.; Vandereerden, J. P. *Nature (London)* **1992**, *356*, 778.
(8) Mansfield, M. L. *Polymer* **1988**, *29*, 1755.
(9) Point, J. J.; Villers, D. *J. Cryst. Growth* **1991**, *114*, 228.
(10) Toda, A. *Polymer* **1991**, *32*, 771.
(11) Frank, F. C. *J. Cryst. Growth* **1974**, *22*, 233.
(12) Seto, T. *Rep. Prog. Polym. Phys. Jpn.* **1964**, *7*, 67.
(13) Kyu, T.; Mehta, R.; Chiu, H.-W. *Phys. Rev. E* **2000**, *61*, 4161.
(14) Toda, A. *Faraday Discuss. Chem. Soc.* **1993**, *95*, 129.
(15) Putra, E. G. R.; Ungar, G. *Macromolecules* **2003**, *36*, 5214.

(16) Ungar, G.; Putra, E. G. R.; de Silva, D. S. M.; Shcherbina, M. A.; Waddon, A. J. *Adv. Polym. Sci.* **2005**, *180*, 45.
(17) Ungar, G.; Putra, E. G. R. *Macromolecules* **2001**, *34*, 5180.
(18) Shcherbina, M. A.; Ungar, G. *Polymer* **2006**, *47*, 5505.
(19) Shcherbina, M. A.; Ungar, G. *Polymer*, submitted for publication.
(20) Toda, A.; Arita, T.; Hikosaka, M. *Polymer* **2001**, *42*, 2223.
(21) Buckley, C. P.; Kovacs, A. J. In *Structure of Crystalline Polymers*; Hall, I. H., Ed.; Elsevier-Applied Science: London, 1984; p 261.
(22) Cheng, S. Z. D.; Chen, J. *J. Polym. Sci., Part B: Polym. Phys.* **1991**, *29*, 311.
(23) Lotz, B.; Kovacs, A. J.; Bassett, G. A.; Keller, A. *Kolloid Z. Z. Polym.* **1966**, *209*, 115.
(24) Ungar, G. In *Polymer Crystallization*; Dosiere, M., Ed.; NATO ASI Series; Kluwer: Dordrecht, 1993.

MA0617872